

Acetate Regulation of Spore Formation Is under the Control of the Ras/Cyclic AMP/Protein Kinase A Pathway and Carbon Dioxide in *Saccharomyces cerevisiae*

Marc Jungbluth, Hans-Ulrich Mösch, and Christof Taxis

Department of Genetics, Philipps-Universität Marburg, Marburg, Germany

In *Saccharomyces cerevisiae*, the Ras/cyclic AMP (cAMP)/protein kinase A (PKA) pathway is a nutrient-sensitive signaling cascade that regulates vegetative growth, carbohydrate metabolism, and entry into meiosis. How this pathway controls later steps of meiotic development is largely unknown. Here, we have analyzed the role of the Ras/cAMP/PKA pathway in spore formation by the meiosis-specific manipulation of Ras and PKA or by the disturbance of cAMP production. We found that the regulation of spore formation by acetate takes place after commitment to meiosis and depends on PKA and appropriate A kinase activation by Ras/Cyr1 adenyl cyclase but not by activation through the Gpa2/Gpr1 branch. We further discovered that spore formation is regulated by carbon dioxide/bicarbonate, and an analysis of mutants defective in acetate transport (*ady2Δ*) or carbonic anhydrase (*nce103Δ*) provided evidence that these metabolites are involved in connecting the nutritional state of the meiotic cell to spore number control. Finally, we observed that the potential PKA target Ady1 is required for the proper localization of the meiotic plaque proteins Mpc70 and Spo74 at spindle pole bodies and for the ability of these proteins to initiate spore formation. Overall, our investigation suggests that the Ras/cAMP/PKA pathway plays a crucial role in the regulation of spore formation by acetate and indicates that the control of meiotic development by this signaling cascade takes place at several steps and is more complex than previously anticipated.

Signal transduction pathways are essential for cells to adjust proliferation, cell size, metabolism, and developmental decisions to external conditions and stimuli. A model used to study these regulatory processes is the sporulation of *Saccharomyces cerevisiae*. Sporulation is induced in diploid cells by starvation for a fermentable carbon source as well as essential nutrients like nitrogen, sulfur, or phosphate and by the presence of a nonfermentable carbon source like acetate. In the course of sporulation, a diploid mother cell transforms into an ascus, which contains up to four ascospores. Sporulation combines meiotic divisions, which produce haploid genomes, with spore formation that leads to the encapsulation of the genetic material protecting it against adverse environmental conditions. Spore formation is initiated during the second meiotic division at the centrosomes (spindle pole bodies [SPBs]) by the formation of a meiosis-specific protein structure called the meiotic plaque (MP), which is composed of the core proteins Mpc54, Mpc70/Spo21, and Spo74 as well as the auxiliary protein Ady4. This structure initiates the fusion of secretory vesicles to form a membrane structure (prospore membrane), which encapsulates parts of the nucleus and cytoplasm. After prospore membrane closure, cytokinesis, and spore wall formation, an ascus is formed, containing four ascospores with a haploid genome (39).

Not only are specific nutrient conditions important to induce sporulation, but cells react to nutrients at all stages of meiosis and spore formation (14). Important steps involving a switch in the capacity to respond to changing nutrient conditions are the commitment to meiosis at the beginning of the first meiotic division and the initiation of spore formation during the metaphase of the second meiotic division. Commitment to meiosis leads to an insulation of the meiotic program against growth-promoting nutrients. Before commitment, the cells abandon meiosis and switch to vegetative growth if they encounter appropriate nutrients,

whereas afterwards, the cells complete meiosis regardless of the nutritional conditions (53). The initiation of spore formation is another important step. Only before this stage are cells able to adjust spore numbers to changes in nutrient availability (57).

The regulation of spore numbers relies on the controlled initiation of MP formation. One part of this regulatory process adapts the amounts of MP components in relation to the available nutrients, limiting these components under starvation conditions. Another part of the regulation is based on differences between the SPBs. MPs are formed preferentially at SPBs, which are created during meiosis and experience fewer cell cycles (15, 40, 57).

How the nutritional status could influence the MP protein abundance or the differences of SPBs has not yet been investigated. It was shown previously that acetate metabolism via the glyoxylate pathway is connected to the regulation of spore numbers (40). Besides this, two proteins are known to be important for the production of large numbers of spores. Ady1 is important for the localization of Mpc54 to SPBs and the formation of MPs (11), whereas Ady2 is important for acetate uptake (44) and MP component production (57). The uptake of acetate raises the pH of the sporulation medium (12); this alkalization is important for the initiation of sporulation (22). The glyoxylate and tricarboxylic acid (TCA) cycles metabolize acetate during sporulation; the main products are carbon dioxide, energy, as well as glutamate at early

Received 16 September 2011 Accepted 22 May 2012

Published ahead of print 1 June 2012

Address correspondence to Christof Taxis, taxis@biologie.uni-marburg.de.

Supplemental material for this article may be found at <http://ec.asm.org/>.

Copyright © 2012, American Society for Microbiology. All Rights Reserved.

doi:10.1128/EC.05240-11

and trehalose at later stages of sporulation (12, 13, 34). In yeast cells, the carbonic anhydrase Nce103 catalyzes the reversible reaction of carbon dioxide and water to proton and bicarbonate (9, 16), with the latter serving as a second messenger which enhances sporulation (19, 20, 42).

Interestingly, a disturbance of spore formation has been observed for mutations affecting the adenylyl cyclase Cyr1 (61), which is part of the Ras/cyclic AMP (cAMP)/protein kinase A (PKA) pathway (67). The adenylyl cyclase Cyr1 synthesizes cAMP, which binds to the regulatory PKA subunit Bcy1. This induces the dissociation of Bcy1 from the catalytic subunit Tpk1, Tpk2, or Tpk3, which results in active PKA. The activity of Cyr1 is stimulated by the small GTP-binding proteins Ras1 and Ras2 as well as the glucose-sensing G-protein-coupled receptor Gpr1 and the α -like protein Gpa2 (67). It is unclear whether the cAMP production of *S. cerevisiae* Cyr1 is stimulated by bicarbonate, as is the case for other fungal adenylyl cyclases (3, 18, 28, 35). Previous *in vitro* studies using adenylyl cyclases suggested that bicarbonate is bound by a lysine within the catalytic center, which is involved in substrate binding (6). Bicarbonate is known to stimulate sporulation in *S. cerevisiae* (19, 20, 42), although it is not known if there is a functional connection to Cyr1. The production of cAMP is counteracted by the 3',5'-cyclic-nucleotide phosphodiesterases Pde1 and Pde2, which hydrolyze cAMP and thereby inactivate PKA (67).

Active PKA regulates target proteins by phosphorylation, thereby influencing cell growth, metabolism, stress resistance, and meiotic entry (54, 56, 67). A high level of activity of PKA is in general connected to vegetative growth, whereas a low level of activity in diploids is a prerequisite for entry into meiosis. The Ras/cAMP/PKA pathway regulates meiotic entry at several steps. Active PKA inhibits the transcription of the two key meiotic regulators *IME1* and *IME2*; additionally, Ime2 is bound by active Gpa2, thereby repressing its kinase activity (22). The transcription factor Ime1 and the kinase Ime2 are both essential for the initiation and progression of sporulation. The activity of PKA during and its influence on meiotic divisions have not been investigated. It is known that cAMP levels rise at the time of meiotic divisions and decrease toward the end of the sporulation process (62). Yeast cells react to growth-promoting nutrients at all stages during sporulation, although there is a difference in the cellular responses before and after commitment. The addition of growth-promoting nutrients before commitment results in a return to vegetative growth; the addition of growth-promoting nutrients after commitment results in a continuation of the sporulation program. Interestingly, this continuation involves a limitation of PKA activity evoked by a strong increase of the *BCY1* expression level (14). This indicates that PKA activity has to be limited to allow the completion of the meiotic divisions and spore formation upon the addition of growth-promoting nutrients. Indeed, the expression of glucose-dependent PKA targets is not upregulated under these conditions (14). The last step in spore biogenesis, the synthesis of mature spore walls, has been found to be influenced by PKA activity via the activation of the meiosis-specific mitogen-activated protein (MAP) kinase homolog Smk1 (33).

The importance of the Ras/cAMP/PKA pathway for meiotic entry has been studied in great detail. However, whether this pathway has essential functions during meiotic divisions or influences sporulation in addition to the initiation of spore wall biogenesis has not been investigated. This lack of knowledge is most likely

due to technical problems in creating Ras/cAMP/PKA pathway component mutants without interfering with vegetative growth or meiotic entry. Here, we used a method which allows the control of Ras/cAMP/PKA pathway activity during meiosis by the destabilization of key components after meiotic entry. The destabilization of target proteins is achieved by the exposure of a dormant N-degron by the site-directed proteolysis of a degradation tag using the tobacco etch virus (TEV) protease (59). The meiosis-specific destabilization of target proteins relies on the usage of the *IME2* promoter for the expression of the TEV protease (27). In the study presented here, we found that meiotic divisions were not affected in mutants with reduced levels of PKA activity. However, we observed that the timing and strength of PKA activity are important for the control of spore numbers. Our results suggest that acetate availability is sensed in part by the amount of carbon dioxide produced in the TCA cycle. Furthermore, we found that the potential PKA target Ady1 controls the ability of MP components to initiate daughter cell formation.

MATERIALS AND METHODS

Yeast strains and plasmids. All yeast strains are derivatives of SK1 strain YKS32 (29) and are listed with their relevant genotypes in Table 1. Chromosomal tagging and gene deletions using PCR products were performed as described previously (26). Briefly, specific primers were used to amplify the selection marker together with the tag; target-gene-specific sequences (40 bases) were present at the 3' end of the primer. After the transformation of the PCR product into yeast, these sequences targeted the PCR product to the selected locus to create a gene fusion or deletion. Template plasmids (pFA6a-kanMX4, pFA6a-hphNT1, and pFA6a-natNT2 for gene deletions; pYM20 for tagging; and pMJ13 and pCT289 for degrons) are listed in Table 2. The correct insertion of the PCR product at the desired open reading frame was checked by PCR using chromosomal DNA as the template. For the creation of a strain carrying *GFP-TD_{eg}F-TPK2* controlled by the *TPK2* promoter, two chromosomal manipulations were performed. First, a construct obtained from pMJ13 (*loxP::URA3::loxP::GFP-TD_{eg}F*) was introduced at the 3' end of *TPK2*. Second, the Cre recombinase was transiently expressed in this strain by using plasmid pSH65. Selection on plates containing 5-fluoroorotic acid allowed us to obtain strains in which the *URA3* marker was removed (17). In general, chromosomal manipulations were carried out with haploid strains; homozygous diploid strains were obtained from crossings and tetrad dissections. The strains used for the depletion of the Ras proteins (YMJ85 and YMJ195), Tpk2 (YMJ209), and Bcy1 (YMJ99 and YMJ221) as well as the corresponding control strains (YMJ79 and YMJ179) contained pDS37 to induce the high-level production of the pTEV⁺ protease during sporulation.

Strains YMJ147, YMJ151, YMJ184, and YMJ181 were derived from a diploid strain with a heterozygous deletion of *CYR1*. Plasmids pMJ15 and pDS66 were transformed into this strain, followed by tetrad dissection and crossing to obtain homozygous diploids. In the case of YMJ184 and YMJ181, *ADY2* was deleted in haploid cells.

Standard preparations of media were used for growth (51). Strains with a deletion of *NCE103* (YMJ132) were grown in a carbon dioxide-enriched atmosphere during strain construction and presporulation growth. Yeast cells were grown in low-fluorescence medium for fluorescence microscopy experiments (58). Plasmids (listed in Table 2) were constructed by standard procedures (2); details and sequences of the vectors used are available upon request.

Microscopy. Live-cell imaging was performed as described previously (27), using a Zeiss Axiovert 200 instrument equipped with a Hamamatsu camera; 4',6-diamidino-2-phenylindole (DAPI), enhanced green fluorescent protein (GFP), and rhodamine filter sets; and a 63 \times Plan Apochromat oil lens (numerical aperture [NA], 1.4). Dif-

TABLE 1 *S. cerevisiae* strains used in this study

Strain	Relevant genotype	Reference
YKS32	<i>MATa/MATα lys2/lys2 ura3/ura3 leu2/LEU2 ho::hisG/ho::LYS</i>	29
LH177	<i>MATa/MATα his3/his3 ura3/ura3 leu2/leu2 trp1/trp1 lys2/lys2 ho::hisG/ho::hisG</i>	24
YMJ79	<i>YKS32 ura3::P_{IME2}-p14^{D122Y}-TEV^{S219V 234STOP}::kanMX/ura3::P_{IME2}-p14^{D122Y}-TEV^{S219V 234STOP}::kanMX</i>	27
YMJ85	<i>YMJ79 natNT2::P_{ADH1}-GFP-TDgF-3HA-RAS1/natNT2::P_{ADH1}-GFP-TDgF-3HA-RAS1 natNT2::P_{ADH1}-GFP-TDgF-3HA-RAS2/natNT2::P_{ADH1}-GFP-TDgF-3HA-RAS2</i>	This work
YMJ179	<i>YKS32 IME2-9Myc::hphNT1/IME2-9Myc::hphNT1</i>	This work
YMJ195	<i>YMJ79 natNT2::P_{ADH1}-GFP-TDgF-3HA-RAS1/natNT2::P_{ADH1}-GFP-TDgF-3HA-RAS1 natNT2::P_{ADH1}-GFP-TDgF-3HA-RAS2/IME2-9Myc::hphNT1/IME2-9Myc::hphNT1</i>	This work
YMJ209	<i>YMJ79 tpk1Δ::natNT2/tpk1Δ::natNT2 tpk3Δ::hphNT1/tpk3Δ::hphNT1 P_{TPK2}-GFP-TDgF-3HA-TPK2/P_{TPK2}-GFP-TDgF-3HA-TPK2</i>	This work
YMJ221	<i>YMJ79 natNT2::P_{ADH1}-GFP-TDgF-3HA-BCY1/natNT2::P_{ADH1}-GFP-TDgF-3HA-BCY1 IME2-9Myc::hphNT1/IME2-9Myc::hphNT1</i>	This work
YMJ99	<i>YMJ79 natNT2::P_{ADH1}-GFP-TDgF-3HA-BCY1/natNT2::P_{ADH1}-GFP-TDgF-3HA-BCY1</i>	This work
YMJ68	<i>YKS32 ady1Δ::natNT2/ady1Δ::natNT2</i>	This work
YMJ69	<i>YKS32 ady2Δ::hphNT1/ady2Δ::hphNT1</i>	This work
YMJ132	<i>YKS32 nce103Δ::hphNT1/nce103Δ::hphNT1</i>	This work
YMJ147	<i>YKS32 cyr1Δ::hphNT1/cyr1Δ::hphNT1 pMJ15 [CYR1 URA3 ARS/CEN]</i>	This work
YMJ151	<i>YKS32 cyr1Δ::hphNT1/cyr1Δ::hphNT1 pDS66 [cyr1^{K1712A} URA3 ARS/CEN]</i>	This work
YMJ184	<i>YKS32 ady2Δ::natNT2/ady2Δ::natNT2 cyr1Δ::hphNT1/cyr1Δ::hphNT1 pMJ15 [CYR1 URA3 ARS/CEN]</i>	This work
YMJ181	<i>YKS32 ady2Δ::natNT2/ady2Δ::natNT2 cyr1Δ::hphNT1/cyr1Δ::hphNT1 pDS66 [cyr1^{K1712A} URA3 ARS/CEN]</i>	This work
YMJ162	<i>YKS32 ady1Δ::natNT2/ady1Δ::natNT2 mpc70Δ::kanMX/MPC70</i>	This work
YAM281	<i>YKS32 MPC70-yeGFP::kanMX/MPC70-yeGFP::kanMX</i>	57
YMJ152	<i>YKS32 ady1Δ::natNT2/ady1Δ::natNT2 MPC70-yeGFP::kanMX/MPC70-yeGFP::kanMX</i>	This work
YMJ161	<i>YKS32 ady1Δ::natNT2/ady1Δ::natNT2 spo74Δ::kanMX/SPO74</i>	This work
YUK63	<i>YKS32 SPO74-yeGFP::kanMX/SPO74-yeGFP::kanMX</i>	57
YMJ153	<i>YKS32 ady1Δ::natNT2/ady1Δ::natNT2 SPO74-yeGFP::kanMX/SPO74-yeGFP::kanMX</i>	This work
YCT775	<i>YKS32 mpc54Δ::kanMX/MPC54 mpc70Δ::kanMX/MPC70 spo74Δ::kanMX/SPO74</i>	57
YCT730	<i>YKS32 MPC54-yeGFP::kanMX/MPC54-yeGFP::kanMX</i>	57
YMJ73	<i>YKS32 ady1Δ::natNT2/ady1Δ::natNT2 MPC54-yeGFP::kanMX/MPC54-yeGFP::kanMX</i>	This work
YMJ160	<i>YKS32 ady1Δ::natNT2/ady1Δ::natNT2 mpc54Δ::kanMX/MPC54</i>	This work
YMJ180	<i>YKS32 gpa2Δ::hphNT1/gpa2Δ::hphNT1</i>	This work
YMJ208	<i>YKS32 gpr1Δ::natNT2/gpr1Δ::natNT2</i>	This work
YDS154	<i>LH177 PDE2-yeGFP::kanMX/PDE2-yeGFP::kanMX</i>	This work
YDS155	<i>LH177 BCY1-yeGFP::kanMX/BCY1-yeGFP::kanMX</i>	This work

ferential interference contrast (DIC) images were collected in a single plane, with fluorescence images as z stacks with 0.3- μ m (for deconvolution) or 0.5- μ m spacing using Volocity image acquisition software (version 5.03; Perkin-Elmer). The deconvolution of the cells shown in Fig. 4 was performed with standard settings in Volocity.

Sporeulation and spore counting. Yeast cells were sporulated in liquid cultures to obtain samples for immunoblotting. Rich medium con-

taining 2% raffinose was used for pregrowth, and cells were washed once with water and resuspended in sporulation (SPO) medium (1, 0.1, or 0.01% potassium acetate in water). Samples were taken at 1-h intervals and subjected to alkaline lysis, TCA precipitation, as well as immunoblotting, as described previously (27). To monitor the progress of sporulation, samples were taken each hour after transfer into SPO medium. The cells were treated with 70% ethanol, washed once with water, suspended in 50% glycerol containing 1 μ g/ml Hoechst 33342, and subjected to fluorescence microscopy. For spore counting, cells were grown on yeast extract-peptone-dextrose (YPD) plates for 48 h. Cells were scratched off the plate, suspended in water, and transferred onto SPO plates (2% agar and 1, 0.1, or 0.01% potassium acetate). The plates were incubated at 30°C for 2 days to complete sporulation. Sporulated cells were treated with 70% ethanol, washed once with water, suspended in 50% glycerol containing 1 μ g/ml Hoechst 33342, and subjected to fluorescence microscopy.

Spore counting was performed by using stacks of images acquired from Hoechst 33342-stained samples. An Axiovert 200 M microscope (Zeiss) equipped with a 63 \times Plan Apochromat oil lens (NA, 1.4; Zeiss), a digital camera (Hamamatsu), and a DAPI filter set (Zeiss) was used for image acquisition by using Volocity software. Maximum projections of the Hoechst 33342 images were superimposed with the phase-contrast image by using ImageJ software (10). The different species of sporulated yeast cells (see Fig. 2B for examples) were discriminated, considering the superimposition of the DIC and Hoechst 33342 images. The sporulation efficiency was calculated as follows: [(% tetrads \times 4) + (% triads \times 3) + (% dyads \times 2) + % monads]/4. The statistical significance of differences in sporulation efficiencies was calculated by using the unpaired *t* test.

TABLE 2 Plasmids used in this study

Plasmid	Relevant genotype	Reference
pRS316	<i>URA3 ARS/CEN</i>	52
B2255	<i>P_{RAS2}-RAS2^{G19V} URA3 ARS/CEN</i>	36
pMJ16	<i>P_{SPS1}-RAS2^{G19V} URA3 ARS/CEN</i>	This work
pMJ17	<i>P_{IME2}-RAS2^{G19V} URA3 ARS/CEN</i>	This work
pDS37	<i>P_{IME2}-GFP-pTEV⁺ URA3 2μm</i>	This work
pCG347	<i>P_{TP1}-3\timesRBD-GFP URA3 ARS/CEN</i>	31
pCG349	<i>P_{TP1}-3\timesRBD-GFP LEU2 2μm</i>	31
pMJ15	<i>CYR1 URA3 ARS/CEN</i>	This work
pDS66	<i>cyr1^{K1712A} URA3 ARS/CEN</i>	This work
pJM13	<i>loxp::klURA3::loxp::GFP-TDgF-SF3B-3HA</i>	This work
pSH65	<i>P_{GAL1}-cre ble^r</i>	17
pCT289	<i>natNT2::P_{ADH1}-GFP-TDgF-SF3B-3HA</i>	59
pFA6a-kanMX6	<i>kanMX4</i>	63
pFA6a-hphNT1	<i>hphNT1</i>	26
pFA6a-natNT2	<i>natNT2</i>	26
pYM20	<i>9myc::hphNT1</i>	26

Experiments with a carbon dioxide-enriched atmosphere, measurement of alkali production, and glycogen staining. To create a carbon dioxide-enriched atmosphere, 2.5-g solid sodium hydrogen carbonate crystals were placed into the lid of an SPO plate and moistened with water. Plates were sealed with adhesive tape and incubated at 30°C for 2 days. Strains with a deletion of *NCE103* (YMJ132) were kept in a carbon dioxide-enriched atmosphere during presporulation growth as well.

The alkalization of the medium was measured by using phenol red-containing SPO plate (1% potassium acetate, 2% agar, 20 mg/liter phenol red) buffered with acetic acid to pH 7. Equal amounts of cells (grown on solid YPD medium) were spotted onto the plates. Images were taken directly after spotting as well as 1 and 7 h later.

Glycogen staining was performed with iodine vapor derived from sublimated iodine (Carl Roth, Karlsruhe, Germany). Equal amounts of yeast cells were spotted onto YPD plates and incubated at 30°C for 2 days. Iodine pellets were added to the lid of the plate. The cell patches were treated with iodine vapors for 5 min. Images of the plate were taken directly before and after treatment.

Immunoblotting. Immunoblotting was performed as described previously (27). Antibodies directed against GFP (Santa Cruz Biotechnology, Santa Cruz, CA), hemagglutinin (HA) (Sigma-Aldrich), and Myc (Santa Cruz Biotechnology, Santa Cruz, CA) as well as horseradish peroxidase (HRPO)-coupled secondary anti-mouse or anti-rabbit antibodies (Dianova, Hamburg, Germany) were used for protein detection. The rabbit anti-tubulin antibody (a kind gift of M. Knop) was used to detect tubulin (loading control).

RESULTS

Ras and PKA are essential for control of spore numbers. We analyzed how the Ras/cAMP/PKA pathway affects meiotic cell divisions and spore formation. For this purpose, we employed a recently developed method that allows the meiosis-specific depletion of proteins (27, 59). Specifically, we created strains that either destabilized both Ras1 and Ras2 (referred to as Ras) during meiosis or contained only a single Tpk subunit, Tpk2, which was depleted accordingly (referred to as Tpk).

First, we analyzed the localization of the fusion proteins under permissive conditions in vegetatively growing cells. We found that Ras proteins localized at the cell periphery (see Fig. S1A in the supplemental material), as expected (31), whereas no clear localization was observed for the Tpk2 fusion protein (data not shown).

Next, we induced sporulation in these strains and observed an almost complete depletion of the Ras proteins or Tpk 2 h after switching to sporulation-inducing conditions at all tested acetate concentrations (Fig. 1A and B). Interestingly, neither the depletion of Ras nor acetate availability affected Ime2 protein levels (Fig. 1A).

We then monitored the timing of meiotic divisions at different acetate concentrations and found that the meiotic divisions were delayed at low acetate concentrations in both control and Ras-depleted cells (Fig. 1C). A small fraction of the Ras-depleted cells appeared to undergo meiotic divisions slightly earlier than the control cells, but the majority of cells with low Ras protein levels were indistinguishable from the control. This shows that acetate availability, but not Ras activity, influences the timing of the meiotic divisions.

Intriguingly, the depletion of Ras or Tpk altered spore formation when amounts of potassium acetate were limiting. More spores were formed in each ascus than in control cells (Fig. 2A). To quantify the sporulation behavior of the mutants, we determined the number of tetrads (4 spores), triads (3 spores), dyads (2

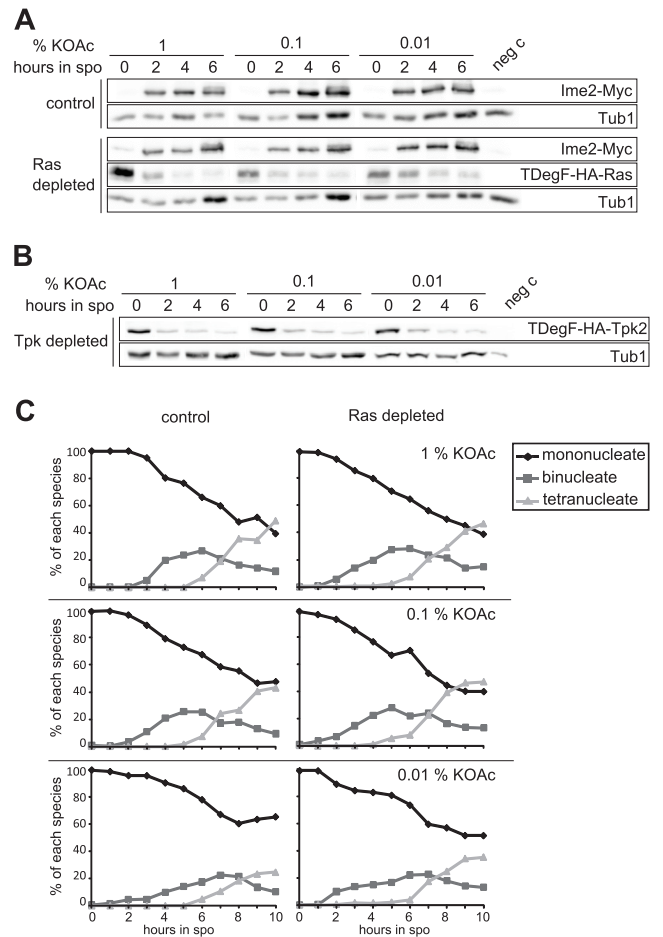


FIG 1 The timing of meiotic cell divisions is influenced by acetate availability but not Ras/cAMP/PKA activity. (A) Immunoblot analysis of cells depleted of Ras1 and Ras2 during sporulation at different acetate concentrations. Samples of control (YMJ179 plus pDS37) and Ras-depleted (YMJ195 plus pDS37) cells were taken at the indicated time points after transfer into sporulation medium (at the potassium acetate [KOAc] concentrations indicated) and subjected to immunoblotting. Antibodies that are specific for HA, Myc, and Tub1 were used to visualize Ras, Ime2, and Tub1, respectively. Antibody specificity was verified by using a wild-type yeast strain (YKS32) as a negative control (neg c). (B) Immunoblot analysis of cells depleted of Tpk2 and deleted for *TPK1* and *TPK3* (YMJ209 plus pDS37) during sporulation at different acetate concentrations. Conditions were as described above for panel A. (C) Time course of meiotic events in control (YMJ79 plus pDS37) and Ras-depleted (YMJ85 plus pDS37) cells sporulating with 1, 0.1, and 0.01% potassium acetate. Hoechst 33342 was used to visualize DNA. The percentages of cells with one (mononucleated), two (binucleated), or four (tetranucleated) DNA signals are given. The graphs show the average data from four independent measurements.

spores), and monads (1 spore). Additionally, the numbers of cells that accomplished the meiotic divisions but produced no spores as well as G_0 cells were taken into account (Fig. 2B). From these data, the sporulation efficiency was calculated, which is a measure of the total number of spores produced in the population. Whereas non-depleted control cells adapted the number of spores in response to acetate availability, Ras- or Tpk-depleted cells almost completely lost this ability and showed a significant increase in levels of spore formation at low acetate concentrations (Fig. 2). This indicates that Ras and PKA activities are essential for the control of spore numbers. We also found that mutants deleted for either *TPK1*,

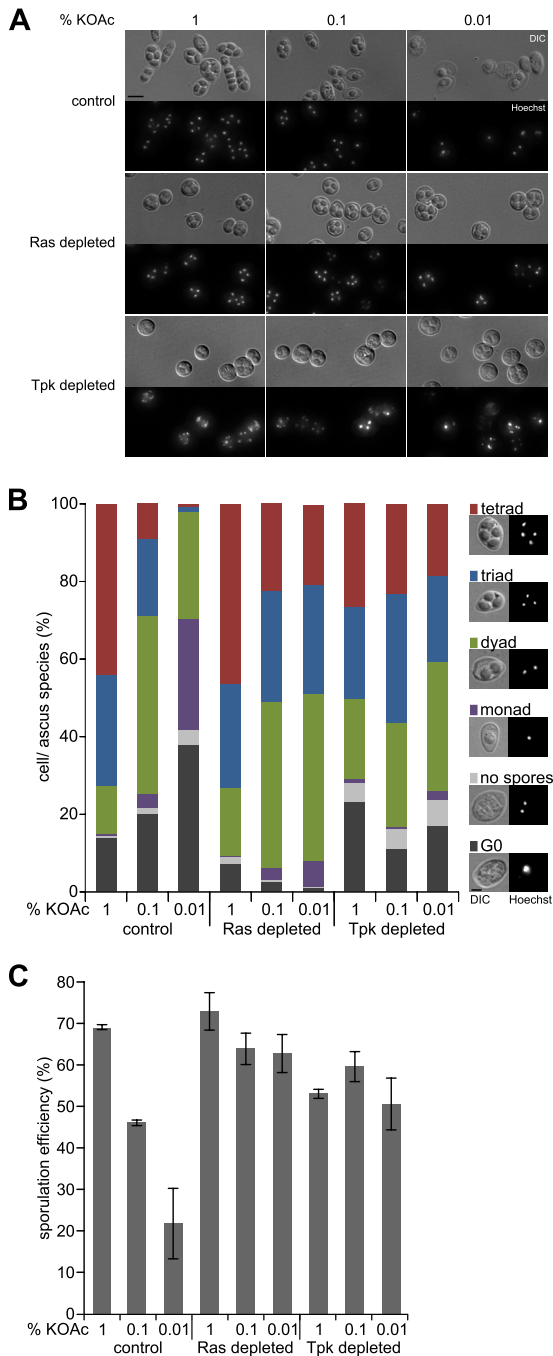


FIG 2 Ras/cAMP/PKA activity is necessary for control of spore numbers. (A) Control cells (YMJ79 plus pDS37) and mutants depleted of Ras (YMJ85 plus pDS37) or Tpk (YMJ209 plus pDS37) were sporulated on plates for 48 h in the presence of 1, 0.1, and 0.01% potassium acetate and stained with Hoechst 33342 to visualize DNA. Bright-field (DIC) and fluorescence (Hoechst) images (maximum-intensity projections) are shown. Bar, 4 μ m. (B) Quantification of spores produced by control cells and mutants depleted of Ras or Tpk sporulated with 1, 0.1, and 0.01% potassium acetate. Spores were counted by using images of sporulated cells (shown in panel A). The different species are shown on the right. Between 100 and 200 cells were assessed for each strain and under each condition. Each strain was measured at least four times. (C) Calculated sporulation efficiencies of control and mutant strains. Error bars indicate standard deviations. The sporulation efficiency directly reflects the number of spores produced by the cells.

TPK2, or *TPK3*, but still expressing the respective two other subunits, behaved like the control strain (data not shown). This finding suggests that no specific catalytic PKA subunit is involved in the control of spore numbers.

Ras and PKA negatively regulate spore formation during meiosis. We next tested the effect of PKA hyperactivation during meiosis by analyzing strains that degrade the regulatory PKA subunit Bcy1 after entry into meiosis. Under permissive conditions, in vegetatively growing cells, the Bcy1 fusion protein was localized mainly in the nucleus (see Fig. S1B in the supplemental material), as expected (25). The depletion of Bcy1 during sporulation resulted in lowered Ime2 protein levels (Fig. 3A). Indeed, it is known that a high level of PKA activity at early stages of meiosis blocks the production of Ime2 (22). Furthermore, we found a decrease in the sporulation efficiency, which was not influenced by acetate availability (Fig. 3B and C). Also, the fraction of nonsporulated cells upon the depletion of Bcy1 was enlarged (see Fig. S1C in the supplemental material), due to the relatively early hyperactivation of PKA. Next, we analyzed how the hyperactivation of the Ras/cAMP/PKA pathway at different meiotic stages affects spore formation. It was previously shown that the expression of the hyperactive *RAS2* allele encoding a G-to-V change at position 19 (*RAS2*^{G19V}) in vegetative cells blocks meiotic initiation almost completely (32). Therefore, we used different promoters to express *RAS2*^{G19V} at different time points after entry into meiosis. Specifically, we used the *IME2* promoter, which is active very early before meiotic commitment, and the promoter of *SPS1*, which is induced after commitment to meiosis (7, 8, 46). We found that the early meiotic expression of *RAS2*^{G19V} resulted in a phenotype that is comparable to that found with *RAS2*^{G19V} expression from the native *RAS2* promoter. Sporulation was almost completely abolished (Fig. 3D and E), and the fraction of nonsporulated G₀ cells was markedly enlarged (see Fig. S1D in the supplemental material). The activation of the Ras/cAMP/PKA pathway after commitment to meiosis by the expression of *RAS2*^{G19V} from the *SPS1* promoter still led to a significant decrease in spore formation. However, this effect was not correlated with an increase in numbers of nonsporulating cells but was correlated with an overall decrease in the number of spores formed per ascus (see Fig. S1D in the supplemental material). Thus, Ras/cAMP/PKA activity affects not only entry into meiosis but also the decision of how many spores are formed by a cell.

Finally, we tested whether the control of spore numbers is affected by Gpa2 or Gpr1, which are known to impinge on PKA activity through the regulation of Cyr1 activity independent of the Ras proteins. However, we found that strains deleted for *GPA2* or *GPR1* did not differ considerably from control strains with respect to spore formation (see Fig. S2A and S2B in the supplemental material), indicating that the Gpr1/Gpa2 input into PKA is not crucial for the control of spore numbers.

In summary, our results demonstrate that the Ras/cAMP/PKA pathway controls sporulation not only before but also after commitment to meiosis. Before commitment, PKA activity regulates entry into meiosis, which has been studied extensively (67). Our data suggest that after commitment, PKA activity is necessary to adapt spore numbers to the availability of nutrients.

Ras activity is not affected by acetate during meiosis. We next wanted to analyze whether the activity of the Ras proteins is affected by acetate during sporulation. Here, we took advantage of an *in vivo* reporter for Ras activity, which consists of the Ras-

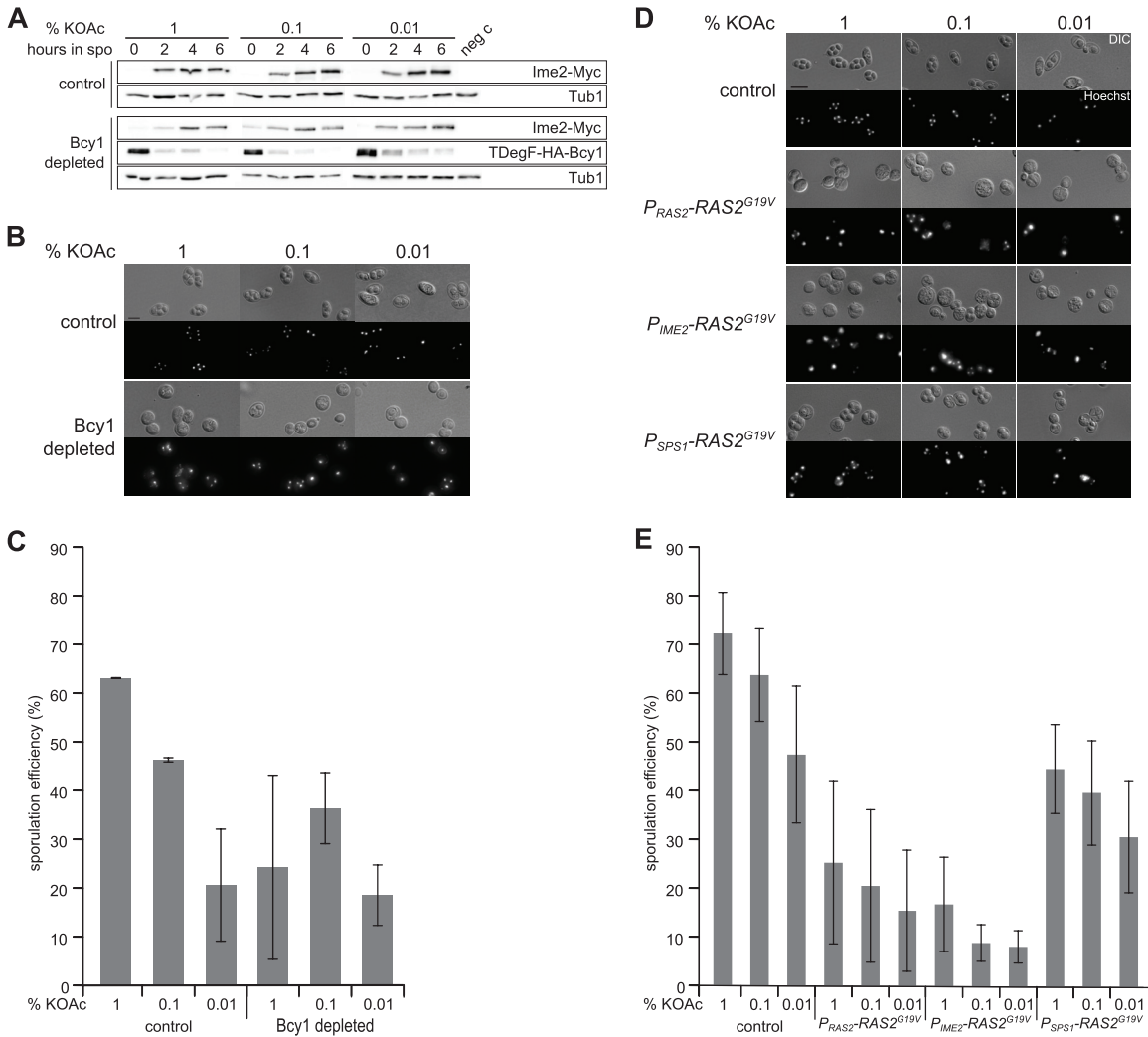


FIG 3 Activation of the Ras/cAMP/PKA pathway leads to a reduction in spore formation. (A) Immunoblot analysis of cells depleted of Bcy1 during sporulation at different acetate concentrations. Samples of control (YMJ79 plus pDS37) and Bcy1-depleted (YMJ221 plus pDS37) cells were taken at the indicated time points after transfer into sporulation medium (at the potassium acetate concentrations indicated) and subjected to immunoblotting. Experimental conditions were as described in the legend of Fig. 1A. (B) Sporulation assay using control cells (YMJ79 plus pDS37) and mutants depleted of Bcy1 (YMJ99 plus pDS37). Conditions were as described in the legend of Fig. 2A. (C) Sporulation efficiency of cells depleted of Bcy1 at different potassium acetate concentrations. Spore counting and quantification were performed as described in the legends of Fig. 2B and C. (D) Control cells (YKS32 plus pRS316) and cells with elevated levels of Ras activity (YKS32 plus B2255 [normal regulation, P_{RAS2} -RAS2^{G19V}], pMJ17 [early expression, P_{IME2} -RAS2^{G19V}], or pMJ16 [expression after commitment, P_{SPS1} -RAS2^{G19V}]) at different times during meiosis were sporulated for 24 h. Experiments were performed as described in the legend of Fig. 2A. Bar, 4 μ m. (E) Quantification of spore production by the strains shown in panel D. Spore counting and quantification were performed as described in the legends of Fig. 2B and C.

binding domain (RBD) of human Raf1 fused to GFP. The GFP-RBD reporter construct binds specifically to active Ras-GTP and allows the detection of changes in Ras activity by live-cell imaging of human and in *S. cerevisiae* cells (1, 31). We found strong GFP-RBD signals in vegetative cells at the cell periphery and in the nucleus (Fig. 4A), as previously reported (31). More importantly, the distribution of GFP-RBD was not altered in sporulating cells, although the signal intensity was slightly reduced. Even mature spores showed a GFP signal at the cell periphery (Fig. 4A). This indicates that significant Ras activity is present during the course of sporulation. The removal of acetate did not change the localization of GFP-RBD (Fig. 4B), suggesting that Ras activity is not influenced by acetate during sporulation. However, the expression of RAS2^{G19V} controlled by the *SPS1* promoter led to a higher

number of cells showing GFP-RBD in the cell periphery, indicating higher levels of Ras activity in these cells during sporulation (see Fig. S2C in the supplemental material). Although Ras is necessary for the control of spore numbers, our results indicate that Ras activity is not modulated in response to changing acetate conditions.

Cyr1 is involved in control of spore numbers. We then addressed the impact of the adenylyl cyclase Cyr1 on the control of spore numbers. Previous *in vitro* and *in vivo* studies with adenylyl cyclases of bacterial and eukaryotic origins showed that a mutation of a lysine residue within the catalytic center involved in substrate binding and bicarbonate responsiveness severely decreases cAMP production (6, 18). We therefore created a corresponding *cyr1*^{K1712A} diploid yeast strain that produces the Cyr1^{K1712A} vari-

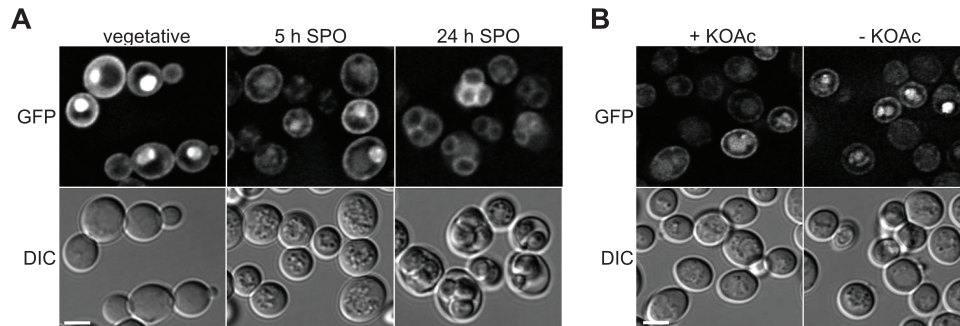


FIG 4 Active Ras is present during the course of sporulation and in mature spores. (A) The localization of 3× RBD-GFP was examined in wild-type cells (YKS32 plus pCG347) during vegetative growth as well as 5 and 24 h after transfer into sporulation medium. Iterative deconvolution was used to process fluorescence images, and single images from the center of the cells are shown (top row). The bottom row shows DIC images. Bar, 4 μ m. (B) The localization of 3× RBD-GFP was observed in wild-type cells 5 h after the induction of sporulation. Images of the cells were taken in the presence of acetate (left column) and 15 min after the removal of SPO medium (right column). Image processing was performed as described above for panel A. The top row shows fluorescence images; the bottom row shows DIC images. Bar, 4 μ m.

ant. The sporulation of this strain revealed a significant increase in levels of spore formation at low acetate levels (Fig. 5A; see also Fig. S3A in the supplemental material), similar to strains that are depleted of Ras or Tpk (Fig. 2B and C). Additionally, we tested whether the increase in the level of spore formation of *cyr1*^{K1712A} cells would persist in an *ADY2* deletion background, in which the ability to form spores is decreased (48). Indeed, we found that the introduction of *cyr1*^{K1712A} in the *ady2* Δ background resulted in an

increased sporulation efficiency (Fig. 5B; see also Fig. S3B in the supplemental material).

Next, we assayed these strains for glycogen formation, which is negatively regulated by PKA activity (67). The presence of the *cyr1*^{K1712A} allele led to an increase in glycogen formation, a characteristic phenotype of cells with low levels of PKA activity (Fig. 5C). However, the removal of *Ady2* did not affect glycogen accumulation in a *CYR1* wild-type background, whereas it increased

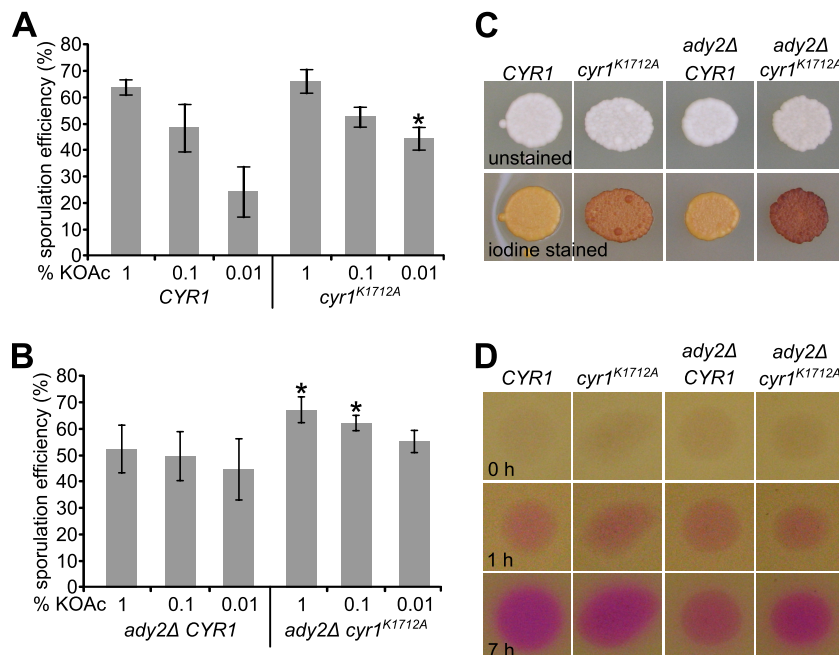


FIG 5 *Cyr1* is involved in spore number control. (A) Sporulation efficiency of control cells (YMJ147) compared to *cyr1*^{K1712A} mutant cells (YMJ151) with 1, 0.1, and 0.01% potassium acetate. Conditions were as described in the legend of Fig. 2C. The increase in the sporulation efficiency with 0.01% potassium acetate was found to be statistically significant (indicated by an asterisk; *P* value of 0.0029 by an unpaired *t* test). (B) Sporulation efficiencies of *ady2* Δ *CYR1* (YMJ184) and *ady2* Δ *cyr1*^{K1712A} (YMJ181) cells with 1, 0.1, and 0.01% potassium acetate. Conditions were as described in the legend of Fig. 2C. Unpaired *t* tests revealed that the increase in the sporulation efficiency of *ady2* Δ *cyr1*^{K1712A} cells is significant for 1% and 0.1% potassium acetate (indicated by an asterisk; *P* values of 0.0095 [1% potassium acetate], 0.018 [0.1% potassium acetate], and 0.0872 [0.01% potassium acetate]). (C) Iodine vapor staining of yeast cells grown in a patch. The top row shows patches before staining; the bottom row shows iodine vapor-treated patches. The same strains as those in panels A and B were used. A darker color of treated patches indicates less PKA activity due to larger amounts of storage carbohydrates in the cells. (D) Alkali production during sporulation of *CYR1* and *ADY2* mutants. Equal amounts of cells were spotted onto SPO plates (pH 7) containing 20 mg/liter phenol red. Images were taken directly after spotting as well as 1 and 7 h later.

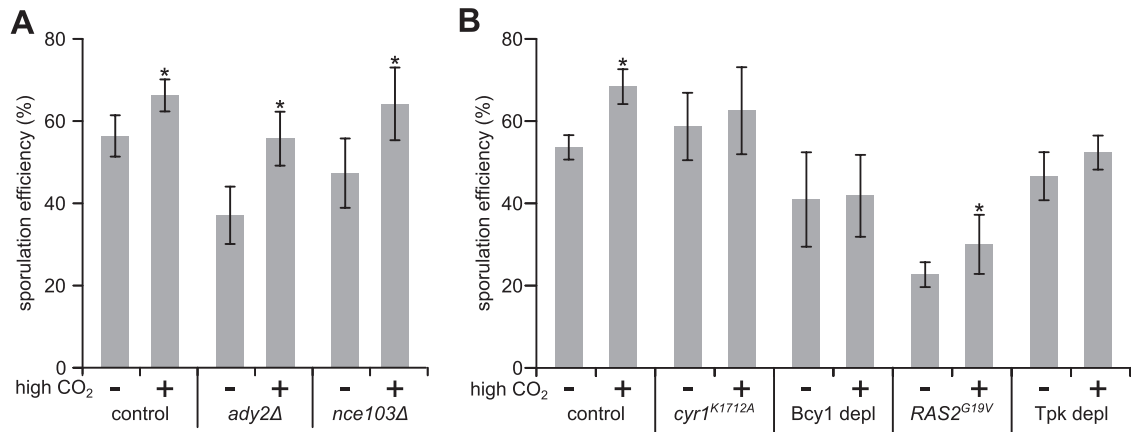


FIG 6 Intracellular formation of bicarbonate is important for efficient sporulation. (A) Sporulation efficiency of control cells (YKS32) and the *ady2Δ* (YMJ69) and *nce103Δ* (YMJ132) mutants (sporulated in the presence of 0.1% potassium acetate) in the absence (–) or presence (+) of a carbon dioxide-enriched atmosphere (high CO₂). Spore counting and quantification were performed as described in the legends of Fig. 2B and C. The increase in the sporulation efficiency was found to be statistically significant for all three strains (indicated by an asterisk; *P* values of 0.0015 [control], 0.0008 [*ady2Δ* mutant], and 0.0016 [*nce103Δ* mutant] by unpaired *t* tests). (B) Sporulation efficiencies of control (YMJ147), *cyr1*^{K1712A} (YMJ151), Bcy1-depleted (YMJ99 plus pDS37), P_{SPS1}-RAS2^{G19V} (YKS32 plus pMJ16), and Tpk-depleted (YMJ209 plus pDS37) cells sporulated in the absence or presence of a carbon dioxide-enriched atmosphere (high CO₂). Conditions were as described above for panel A. Changes in the sporulation efficiency were found to be statistically significant for control and RAS2^{G19V} cells (indicated by an asterisk; *P* values of 0.0012 and 0.0182, respectively, by unpaired *t* tests), whereas the differences for the other strains were not significant (*P* values of 0.4994 for *cyr1*^{K1712A} cells, 0.8723 for Bcy1-depleted cells, and 0.4166 for Tpk-depleted cells).

accumulation in the *cyr1*^{K1712A} mutant strain. We also measured the alkalization of the medium during sporulation by phenol red staining to test the different yeast strains for their capacities to metabolize acetate (12, 45). The *ady2Δ* mutant strain was found to have a lower capacity to metabolize acetate than the control strain (Fig. 5D). During sporulation in liquid cultures, we found a similar behavior, as the increase of the pH was less pronounced in *ady2Δ* cultures than in a control strain (data not shown). Interestingly, the introduction of the *cyr1*^{K1712A} mutation in the *ady2Δ* background led to an increase in alkalization, indicating that a low level of Cyr1 activity rescues not only the sporulation defect but also the defect in acetate metabolism. Overall, our data demonstrate the involvement of Cyr1 in the control of spore numbers and Ady2-mediated alkalization, indicating a functional relationship between these two proteins.

Sporulation efficiency is affected by intracellular carbon dioxide/bicarbonate. We next wanted to know whether intracellular bicarbonate levels are important for sporulation. Bicarbonate has been shown to act as an extracellular factor that promotes meiosis and sporulation by the alkalization of the medium (19, 20, 42) as well as a regulator of a specific group of fungal adenylyl cyclases (3, 18, 28, 35). However, it is not known whether bicarbonate has an intracellular role during the sporulation of *S. cerevisiae*. Therefore, we tested how a carbon dioxide-enriched atmosphere that raises intracellular bicarbonate levels affects spore formation in a control strain and in strains that lack either the plasma membrane-located acetate transporter Ady2 or the carbonic anhydrase Nce103. At regular carbon dioxide concentrations, both mutant strains showed a reduction in the sporulation efficiency compared to that of control cells (Fig. 6A), a finding which was expected for the strain lacking Ady2 (48). However, this effect was less pronounced in *nce103Δ* mutants than in the *ady2Δ* strain. We observed a general increase in sporulation efficiency for all three strains under a carbon dioxide-enriched atmosphere (Fig. 6A). However, this positive effect of carbon dioxide was observed

only in the presence of large or medium amounts of potassium acetate but not at very low acetate levels (data not shown). A further quantification of the cell and ascus species revealed that a carbon dioxide-enriched atmosphere led to an increase in the number of tetrads and a decrease in the number of dyads in both the *nce103Δ* and *ady2Δ* mutant strains (see Fig. S3C in the supplemental material). We also assessed the impact of a carbon dioxide-enriched atmosphere on sporulation in a strain lacking Ady1, which is required for efficient spore formation by influencing MP formation (11). In *ady1* mutants, however, carbon dioxide levels did not affect the sporulation efficiency, which was also found for mutants that had a reduced level of production of MP components (data not shown). This finding suggests that bicarbonate-dependent regulation acts upstream of MP formation.

We then investigated how mutants of the Ras/cAMP/PKA pathway respond to the presence of large amounts of carbon dioxide during sporulation. Interestingly, all tested strains showed an increase in the number of spores per ascus, although this effect was not very pronounced in strains producing Cyr1^{K1712A} or depleted of Tpk or Bcy1 (see Fig. S3D in the supplemental material). The quantification of the sporulation efficiencies of these strains revealed a significant carbon dioxide-induced increase only in control and Ras2^{G19V} cells (Fig. 6B). Moreover, we were interested to know whether PKA activity is influenced by nutrient conditions or bicarbonate. It was reported previously that the abundance and localization of Pde2 are under the control of PKA activity (23) and that the abundance and localization of Bcy1 react to changes in nutritional conditions (60). However, we did not find changes in the localization or abundance of Pde2-GFP and Bcy1-GFP upon the removal of acetate or upon the addition of bicarbonate during sporulation (see Fig. S4A to S4E in the supplemental material). In addition, we measured cAMP levels at the time of meiotic divisions in cells exposed or not exposed to bicarbonate but did not observe differences in cAMP concentrations (data not shown). Taken together, our findings indicate that carbon dioxide and/or

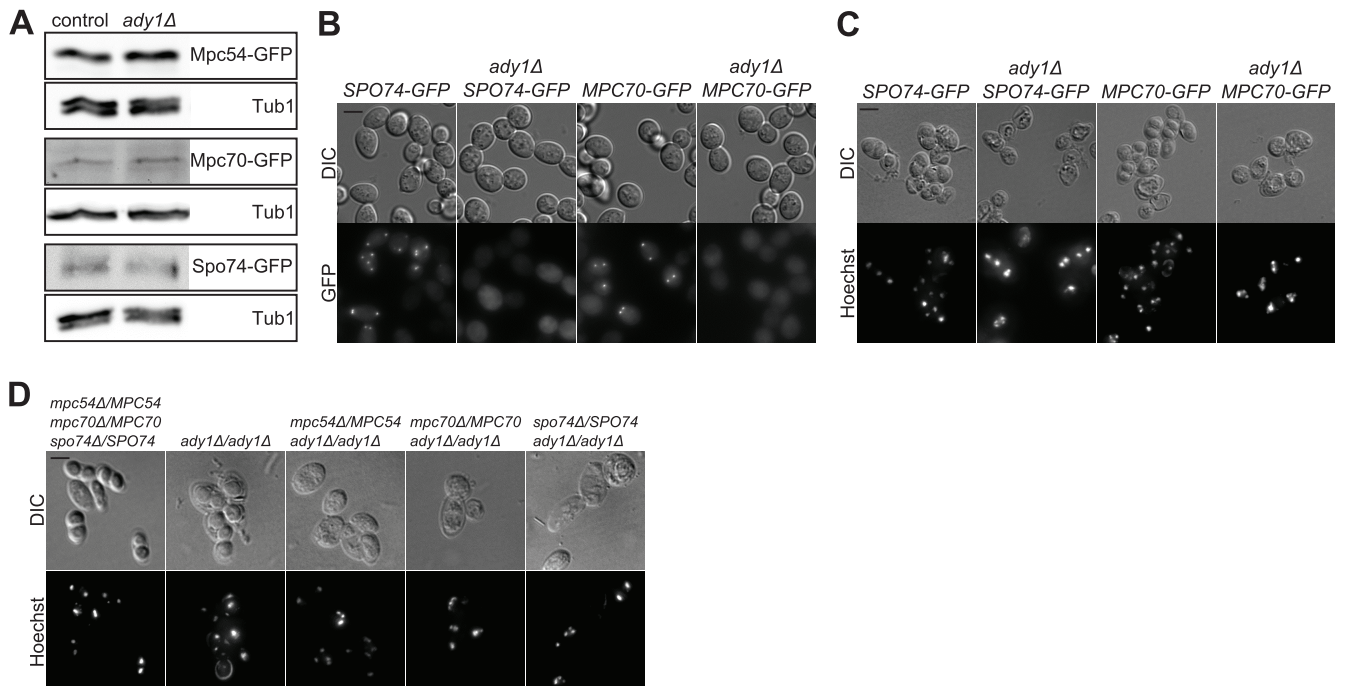


FIG 7 Genetic interaction between *ADY1* and genes encoding MP components. (A) *Ady1* does not influence the abundance of MP proteins. Samples of the cells (strains YCT730, YMJ73, YAM281, YMJ152, YUK63, and YMJ153) were collected at 1-h intervals (4 to 10 h) after a shift to sporulation medium and subjected to alkaline/TCA lysis. Samples of each strain were pooled and used for immunoblot analysis using GFP-specific antibodies. Tub1 was detected to control for loading differences. (B) *Spo74-GFP* and *Mpc70-GFP* do not bind to SPBs in the absence of *Ady1*. Average intensities (GFP channel) and DIC images of cells during sporulation (8 h after transfer into sporulation medium) are shown. The same strains as those in panel A were used. (C) Deletion of *ADY1* in *SPO74-GFP* or *MPC70-GFP* (chromosomally integrated) cells inhibits spore formation. Cells were sporulated for 48 h and stained with Hoechst 33342. Fluorescence and DIC images are shown. Bar, 4 μ m. (D) *ADY1* is essential for spore formation in strains carrying heterozygous knockouts of MP component genes (YCT775, YMJ68, YMJ160, YMJ162, and YMJ161). Conditions were as described above for panel C.

bicarbonate positively affects spore formation, but we did not find evidence that *Cyr1* and, thereby, PKA activity are influenced by CO_2 /bicarbonate.

The potential PKA target protein *Ady1* affects localization of MP components. We then addressed the question of how PKA might control spore formation. Specifically, we investigated how the potential PKA target protein *Ady1* affects MP components. Previously, it was shown that *Ady1* is phosphorylated by the PKA subunit *Tpk3* *in vitro* (47) and is involved in MP formation by influencing the localization of *Mpc54* at SPBs (11). To analyze the impact of *Ady1* on the levels of all known essential MP components, we expressed *MPC54-GFP*, *MPC70-GFP*, and *SPO74-GFP* fusions in control and *ady1* Δ strains. We found that the absence of *Ady1* did not affect the abundance of any of the three MP components (Fig. 7A). However, live-cell imaging revealed that *Mpc70-GFP* and *Spo74-GFP* lost their colocalization with the SPB in the absence of *Ady1* (Fig. 7B). This finding suggests that *Ady1* influences the ability of all known essential MP components to bind to the SPB.

We also observed that the fusion of GFP to *Mpc70* and *Spo74* negatively affects spore formation, as previously described (4). This effect was significantly exacerbated in *ady1* Δ mutant strains, in which spore formation was fully blocked, although meiotic cell divisions were not disturbed in these cells (Fig. 7C). To further investigate the relationship between *Ady1* and the MP components, we introduced heterozygous deletions of *MPC54*, *MPC70*, or *SPO74* in a diploid *ady1* Δ strain. It was shown previously that a

reduction in the number of MP components results in fewer spores per ascus (4, 41, 57, 65). Here, we found that heterozygous deletions of MP component genes in *ady1* Δ cells also exacerbated sporulation defects, further supporting a functional relationship between *Ady1* and the MP (Fig. 7D). In summary, these data indicate that *Ady1* controls the localization and activity of MP components and potentially links the PKA pathway to spore formation.

DISCUSSION

In this study, we have investigated the role of the Ras/cAMP/PKA pathway in the sporulation of *S. cerevisiae*. Previous studies have clearly shown that the activation of this signaling pathway negatively affects entry into meiosis and spore formation (22, 54, 67). Here, we find that the pathway also regulates sporulation after entry into this developmental process. Specifically, we have shown that the pathway controls spore formation after commitment to meiosis and is required for the regulation of spore numbers by acetate availability. Finally, we found that the potential PKA target protein *Ady1* plays a crucial role in localizing several MP components to the SPB, thereby providing a molecular link between PKA and sporulation. As such, our study suggests that the Ras/cAMP/PKA pathway controls meiosis and spore formation by mechanisms that are far more complex than previously anticipated.

One crucial question is the time point(s) after commitment when the Ras/cAMP/PKA pathway exerts its control on meiotic events. Before commitment, a high level of PKA activity leads to

the abandonment of meiosis and return to growth (53). However, measurements of cAMP levels during sporulation and mutational analyses of Ras/cAMP/PKA pathway components (33, 61, 62, 64) have suggested that PKA is active during a longer period after meiotic entry. Moreover, a negative-feedback loop relying on the expression of *BCY1* prevents very high levels of activity of PKA after commitment to meiosis (14). It was shown previously that the adaptation of spore numbers in response to acetate availability is performed at the level of MP formation, which takes place during the transition from anaphase meiosis I to metaphase meiosis II (57). Our present work supports a crucial role for PKA during sporulation, and the findings indicate that PKA activity influences spore numbers after commitment. Therefore, the time between these two events (commitment and MP formation) seems to be crucial for the regulation of spore numbers.

A further concern is the mechanism by which the Ras/cAMP/PKA pathway controls MP formation. In principle, PKA activity might control the abundance and/or activity of MP components. A direct influence on MP formation is established through the transcription factor Ime1, which is well known to be regulated by PKA and which controls the expression of early meiotic genes together with the DNA-binding protein Ume6 (22). The gene encoding the MP component Mpc54 was classified as an early meiotic gene belonging to the core set of genes regulated by Ume6 (7, 66). Moreover, it has been found that the expression levels of *ADY2*, *MPC54*, and *MPC70/SPO21* are diminished upon the transfer of sporulation-committed cells to growth-promoting medium containing glucose (14). Altogether, this suggests that PKA also controls the expression of genes encoding MP components after commitment. Still unknown are the exact mechanism as well as the whole set of transcription factors involved in the adaptation to changing nutrient conditions during sporulation. In addition, PKA might also control the abundance of MP components by a global regulatory mechanism, e.g., through a general regulation of RNA polymerase II activity or the control of ribosome biogenesis and subsequent protein synthesis (5, 67). However, we did not find that control proteins like Ime2 and Tub1 change their abundance by varying the acetate concentrations (Fig. 1A and 3A), suggesting a more specific control mechanism. Finally, our study provides evidence that PKA might regulate the abundance as well as the activity of MP components, since the potential PKA target protein *Ady1* is necessary not only for MP formation (11) but also for the localization of all essential MP components at SPBs. It will be interesting to see how exactly PKA controls *Ady1* activity *in vivo* and how this affects the formation of MPs.

Another way in which PKA controls the sporulation efficiency seems to be through metabolic adaptations. The A kinase is well known to regulate carbohydrate metabolism and to influence the mitochondrial respiratory capacity as well as the abundance and activity of glyoxylate and TCA cycle enzymes in vegetative cells (21, 30, 43, 47, 49, 50, 55, 67). Thus, PKA-induced metabolic changes might also affect energy production during meiosis and spore formation. Indeed, it was shown previously that an intermediary metabolite of the glyoxylate cycle is important for the production of high numbers of spores (40). Our results suggest that carbon dioxide, which is a metabolite produced during the metabolism of acetate from the TCA cycle and which is converted to bicarbonate by *Nce103*, serves as a second measure of the respiratory capacity that affects the sporulation efficiency. Surprisingly, a

carbon dioxide-enriched atmosphere had no influence on sporulation behavior at low acetate concentrations (data not shown). Possibly, small amounts of the glyoxylate cycle metabolite do not allow efficient sporulation under these conditions. However, we found high numbers of spores in strains with decreased levels of PKA activity under such conditions, which might result from a relief of the PKA-dependent inhibition of TCA and glyoxylate cycle activity as well as an increased ability to form MPs. This might also explain the reversion of phenotypes in the *ady2Δ* strain upon the mutation of *CYR1*. Overall, yeast cells seem to enter meiosis with enough energy to form triads and tetrads even if exposed to small amounts of acetate, but the adaptation of spore numbers might be a way to save nutrients for long-term survival. Indeed, the storage carbohydrate trehalose is one of the main products of acetate metabolism during sporulation (12). Bicarbonate-dependent communication between yeast cells and the alkalization of the sporulation medium demonstrate the importance of extracellular carbon dioxide (19, 20, 42). Our finding that increases in levels of carbon dioxide rescue the sporulation defect of an *ady2Δ* mutant underscores the importance of this TCA cycle intermediate. This result, together with the observation that carbonic anhydrase is important for efficient sporulation, argues for a crucial intracellular role of carbon dioxide/bicarbonate.

It is interesting to compare the roles of the Ras/cAMP/PKA pathway during mitotic and meiotic cell division. Similar to its role during mitosis (54, 67), we found that the pathway is involved in the transduction of nutritional signals during meiosis. However, not all components of the pathway are required during mitosis and meiosis or seem to act in the same way. Whereas the Ras proteins appear to be required for the basal activation of *Cyr1* during mitosis and meiosis, the activation of the adenylyl cyclase by the *Gpa2/Gpr1* branch is not important for the control of spore numbers. Moreover, Ras activity rapidly changes in response to changes in nutrient availability during vegetative growth (67). However, our study did not reveal differences in Ras or PKA activity in the presence or absence of acetate during meiosis. The differential nutritional regulation of Ras proteins during mitosis and meiosis might be achieved by differential activation through guanine nucleotide exchange factors (GEFs). Interestingly, previous domain analyses of the Ras GEF *Cdc25* have shown that distinct domains of the protein are essential for its activity during vegetative growth and sporulation (37, 38). Future detailed analyses of the Ras/cAMP/PKA pathway during sporulation might therefore uncover further crucial differences between its mitotic and meiotic functions and help us to understand how regulatory circuits are adapted to different nutritional signals and environmental conditions.

ACKNOWLEDGMENTS

We thank Campbell Gourlay for plasmids, Michael Knop for reagents, and Roberta Spadaccini for helpful comments on the manuscript. We are grateful to Johannes Freitag and all members of the Mösch group for fruitful discussions. We acknowledge Daniela Störmer for her excellent technical assistance.

M.J. was supported by DFG grant GK1216, Intra and Intercellular Transport and Communication.

REFERENCES

1. Augsten M, et al. 2006. Live-cell imaging of endogenous Ras-GTP illustrates predominant Ras activation at the plasma membrane. *EMBO Rep.* 7:46–51.

2. Ausubel FM, et al. 1995. Current protocols in molecular biology. John Wiley & Sons, New York, NY.
3. Bahn YS, Cox GM, Perfect JR, Heitman J. 2005. Carbonic anhydrase and CO₂ sensing during *Cryptococcus neoformans* growth, differentiation, and virulence. *Curr. Biol.* 15:2013–2020.
4. Bajjarg BK, Malzone M, Nickas M, Neiman AM. 2001. SPO21 is required for meiosis-specific modification of the spindle pole body in yeast. *Mol. Biol. Cell* 12:1611–1621.
5. Bjorklund S, Gustafsson CM. 2005. The yeast Mediator complex and its regulation. *Trends Biochem. Sci.* 30:240–244.
6. Cann MJ, Hammer A, Zhou J, Kanacher T. 2003. A defined subset of adenylyl cyclases is regulated by bicarbonate ion. *J. Biol. Chem.* 278:35033–35038.
7. Chu S, et al. 1998. The transcriptional program of sporulation in budding yeast. *Science* 282:699–705.
8. Chu S, Herskowitz I. 1998. Gametogenesis in yeast is regulated by a transcriptional cascade dependent on Ndt80. *Mol. Cell* 1:685–696.
9. Clark D, Rowlett RS, Coleman JR, Klessig DF. 2004. Complementation of the yeast deletion mutant deltaNCE103 by members of the beta class of carbonic anhydrases is dependent on carbonic anhydrase activity rather than on antioxidant activity. *Biochem. J.* 379:609–615.
10. Collins TJ. 2007. ImageJ for microscopy. *Biotechniques* 43:25–30.
11. Deng C, Saunders WS. 2001. ADY1, a novel gene required for prospore membrane formation at selected spindle poles in *Saccharomyces cerevisiae*. *Mol. Biol. Cell* 12:2646–2659.
12. Dickinson JR, Dawes IW, Boyd AS, Baxter RL. 1983. ¹³C NMR studies of acetate metabolism during sporulation of *Saccharomyces cerevisiae*. *Proc. Natl. Acad. Sci. U. S. A.* 80:5847–5851.
13. Esposito MS, Esposito RE, Arnaud M, Halvorson HO. 1969. Acetate utilization and macromolecular synthesis during sporulation of yeast. *J. Bacteriol.* 100:180–186.
14. Friedlander G, et al. 2006. Modulation of the transcription regulatory program in yeast cells committed to sporulation. *Genome Biol.* 7:R20. doi:10.1186/gb-2006-7-3-r20.
15. Gordon O, et al. 2006. Nud1p, the yeast homolog of Centriolin, regulates spindle pole body inheritance in meiosis. *EMBO J.* 25:3856–3868.
16. Gotz R, Gnann A, Zimmermann FK. 1999. Deletion of the carbonic anhydrase-like gene NCE103 of the yeast *Saccharomyces cerevisiae* causes an oxygen-sensitive growth defect. *Yeast* 15:855–864.
17. Gueldener U, Heinisch J, Koehler GJ, Voss D, Hegemann JH. 2002. A second set of loxP marker cassettes for Cre-mediated multiple gene knock-outs in budding yeast. *Nucleic Acids Res.* 30:e23. doi:10.1093/nar/30.6.e23.
18. Hall RA, et al. 2010. CO₂ acts as a signalling molecule in populations of the fungal pathogen *Candida albicans*. *PLoS Pathog.* 6:e1001193. doi:10.1371/journal.ppat.1001193.
19. Hayashi M, Ohkuni K, Yamashita I. 1998. Control of division arrest and entry into meiosis by extracellular alkalinisation in *Saccharomyces cerevisiae*. *Yeast* 14:905–913.
20. Hayashi M, Ohkuni K, Yamashita I. 1998. An extracellular meiosis-promoting factor in *Saccharomyces cerevisiae*. *Yeast* 14:617–622.
21. Hedbacker K, Townley R, Carlson M. 2004. Cyclic AMP-dependent protein kinase regulates the subcellular localization of Snf1-Sip1 protein kinase. *Mol. Cell. Biol.* 24:1836–1843.
22. Honigberg SM, Purnapatre K. 2003. Signal pathway integration in the switch from the mitotic cell cycle to meiosis in yeast. *J. Cell Sci.* 116:2137–2147.
23. Hu Y, Liu E, Bai X, Zhang A. 2010. The localization and concentration of the PDE2-encoded high-affinity cAMP phosphodiesterase is regulated by cAMP-dependent protein kinase A in the yeast *Saccharomyces cerevisiae*. *FEMS Yeast Res.* 10:177–187.
24. Huang LS, Doherty HK, Herskowitz I. 2005. The Smk1p MAP kinase negatively regulates Gsc2p, a 1,3-beta-glucan synthase, during spore wall morphogenesis in *Saccharomyces cerevisiae*. *Proc. Natl. Acad. Sci. U. S. A.* 102:12431–12436.
25. Huh WK, et al. 2003. Global analysis of protein localization in budding yeast. *Nature* 425:686–691.
26. Janke C, et al. 2004. A versatile toolbox for PCR-based tagging of yeast genes: new fluorescent proteins, more markers and promoter substitution cassettes. *Yeast* 21:947–962.
27. Jungbluth M, Renicke C, Taxis C. 2010. Targeted protein depletion in *Saccharomyces cerevisiae* by activation of a bidirectional degen. *BMC Syst. Biol.* 4:176.
28. Klengel T, et al. 2005. Fungal adenylyl cyclase integrates CO₂ sensing with cAMP signaling and virulence. *Curr. Biol.* 15:2021–2026.
29. Knop M, Strasser K. 2000. Role of the spindle pole body of yeast in mediating assembly of the prospore membrane during meiosis. *EMBO J.* 19:3657–3667.
30. Leadsham JE, Gourelay CW. 2010. cAMP/PKA signaling balances respiratory activity with mitochondria dependent apoptosis via transcriptional regulation. *BMC Cell Biol.* 11:92. doi:10.1186/1471-2121-11-92.
31. Leadsham JE, et al. 2009. Whi2p links nutritional sensing to actin-dependent Ras-cAMP-PKA regulation and apoptosis in yeast. *J. Cell Sci.* 122:706–715.
32. Matsuura A, et al. 1990. The adenylyl cyclase/protein kinase cascade regulates entry into meiosis in *Saccharomyces cerevisiae* through the gene IME1. *EMBO J.* 9:3225–3232.
33. McDonald CM, et al. 2009. The Ras/cAMP pathway and the CDK-like kinase Ime2 regulate the MAPK Smk1 and spore morphogenesis in *Saccharomyces cerevisiae*. *Genetics* 181:511–523.
34. Miyake S, Sando N, Sato S. 1971. Biochemical changes in yeast during sporulation. II. Acetate metabolism. *Dev. Growth Differ.* 12:285–296.
35. Mogensen EG, et al. 2006. *Cryptococcus neoformans* senses CO₂ through the carbonic anhydrase Can2 and the adenylyl cyclase Cac1. *Eukaryot. Cell* 5:103–111.
36. Mosch HU, Roberts RL, Fink GR. 1996. Ras2 signals via the Cdc42/Ste20/mitogen-activated protein kinase module to induce filamentous growth in *Saccharomyces cerevisiae*. *Proc. Natl. Acad. Sci. U. S. A.* 93:5352–5356.
37. Munder T, Kuntzel H. 1989. Glucose-induced cAMP signaling in *Saccharomyces cerevisiae* is mediated by the CDC25 protein. *FEBS Lett.* 242:341–345.
38. Munder T, Mink M, Kuntzel H. 1988. Domains of the *Saccharomyces cerevisiae* CDC25 gene controlling mitosis and meiosis. *Mol. Gen. Genet.* 214:271–277.
39. Neiman AM. 2005. Ascospore formation in the yeast *Saccharomyces cerevisiae*. *Microbiol. Mol. Biol. Rev.* 69:565–584.
40. Nickas ME, Diamond AE, Yang MJ, Neiman AM. 2004. Regulation of spindle pole function by an intermediary metabolite. *Mol. Biol. Cell* 15:2606–2616.
41. Nickas ME, Schwartz C, Neiman AM. 2003. Ady4p and Spo74p are components of the meiotic spindle pole body that promote growth of the prospore membrane in *Saccharomyces cerevisiae*. *Eukaryot. Cell* 2:431–445.
42. Ohkuni K, Hayashi M, Yamashita I. 1998. Bicarbonate-mediated social communication stimulates meiosis and sporulation of *Saccharomyces cerevisiae*. *Yeast* 14:623–631.
43. Ordiz I, Herrero P, Rodicio R, Moreno F. 1996. Glucose-induced inactivation of isocitrate lyase in *Saccharomyces cerevisiae* is mediated by the cAMP-dependent protein kinase catalytic subunits Tpk1 and Tpk2. *FEBS Lett.* 385:43–46.
44. Paiva S, Devaux F, Barbosa S, Jacq C, Casal M. 2004. Ady2p is essential for the acetate permease activity in the yeast *Saccharomyces cerevisiae*. *Yeast* 21:201–210.
45. Piccirillo S, White MG, Murphy JC, Law DJ, Honigberg SM. 2010. The Rim101p/PacC pathway and alkaline pH regulate pattern formation in yeast colonies. *Genetics* 184:707–716.
46. Primig M, et al. 2000. The core meiotic transcriptome in budding yeasts. *Nat. Genet.* 26:415–423.
47. Ptacek J, et al. 2005. Global analysis of protein phosphorylation in yeast. *Nature* 438:679–684.
48. Rabitsch KP, et al. 2001. A screen for genes required for meiosis and spore formation based on whole-genome expression. *Curr. Biol.* 11:1001–1009.
49. Roosen J, et al. 2005. PKA and Sch9 control a molecular switch important for the proper adaptation to nutrient availability. *Mol. Microbiol.* 55:862–880.
50. Schneper L, Duvel K, Broach JR. 2004. Sense and sensibility: nutritional response and signal integration in yeast. *Curr. Opin. Microbiol.* 7:624–630.
51. Sherman F. 2002. Getting started with yeast. *Methods Enzymol.* 350:3–41.
52. Sikorski RS, Hieter P. 1989. A system of shuttle vectors and yeast host strains designed for efficient manipulation of DNA in *Saccharomyces cerevisiae*. *Genetics* 122:19–27.
53. Simchen G. 2009. Commitment to meiosis: what determines the mode of division in budding yeast? *Bioessays* 31:169–177.

54. Smets B, et al. 2010. Life in the midst of scarcity: adaptations to nutrient availability in *Saccharomyces cerevisiae*. *Curr. Genet.* **56**:1–32.
55. Swiegers JH, Pretorius IS, Bauer FF. 2006. Regulation of respiratory growth by Ras: the glyoxylate cycle mutant, *cit2Delta*, is suppressed by *RAS2*. *Curr. Genet.* **50**:161–171.
56. Tamaki H. 2007. Glucose-stimulated cAMP-protein kinase A pathway in yeast *Saccharomyces cerevisiae*. *J. Biosci. Bioeng.* **104**:245–250.
57. Taxis C, et al. 2005. Spore number control and breeding in *Saccharomyces cerevisiae*: a key role for a self-organizing system. *J. Cell Biol.* **171**:627–640.
58. Taxis C, et al. 2006. Dynamic organization of the actin cytoskeleton during meiosis and spore formation in budding yeast. *Traffic* **7**:1628–1642.
59. Taxis C, Stier G, Spadaccini R, Knop M. 2009. Efficient protein depletion by genetically controlled deprotection of a dormant N-degron. *Mol. Syst. Biol.* **5**:267.
60. Tudisca V, et al. 2010. Differential localization to cytoplasm, nucleus or P-bodies of yeast PKA subunits under different growth conditions. *Eur. J. Cell Biol.* **89**:339–348.
61. Uno I, Matsumoto K, Hirata A, Ishikawa T. 1985. Outer plaque assembly and spore encapsulation are defective during sporulation of adenylate cyclase-deficient mutants of *Saccharomyces cerevisiae*. *J. Cell Biol.* **100**:1854–1862.
62. Uno I, Oshima T, Hirata A, Ishikawa T. 1990. The functional domain of adenylate cyclase associated with entry into meiosis in *Saccharomyces cerevisiae*. *J. Bacteriol.* **172**:102–109.
63. Wach A, Brachat A, Pohlmann R, Philippsen P. 1994. New heterologous modules for classical or PCR-based gene disruptions in *Saccharomyces cerevisiae*. *Yeast* **10**:1793–1808.
64. Watson DC, Berry DR. 1977. Fluctuation in the levels of intracellular and extracellular cAMP during sporulation in *Saccharomyces cerevisiae*. *FEMS Microbiol. Lett.* **1**:83–86.
65. Wesp A, Prinz S, Fink GR. 2001. Conservative duplication of spindle poles during meiosis in *Saccharomyces cerevisiae*. *J. Bacteriol.* **183**:2372–2375.
66. Williams RM, et al. 2002. The Ume6 regulon coordinates metabolic and meiotic gene expression in yeast. *Proc. Natl. Acad. Sci. U. S. A.* **99**:13431–13436.
67. Zaman S, Lippman SI, Zhao X, Broach JR. 2008. How *Saccharomyces* responds to nutrients. *Annu. Rev. Genet.* **42**:27–81.